

# UC Santa Cruz

## UC Santa Cruz Previously Published Works

### Title

Carbohydrate -actuated nanofluidic diode: switchable current rectification in a nanopipette

### Permalink

<https://escholarship.org/uc/item/2k44t43p>

### Journal

Nanoscale, 5(19)

### ISSN

2040-3364

### Authors

Vilozny, Boaz  
Wollenberg, Alexander L  
Actis, Paolo  
et al.

### Publication Date

2013

### DOI

10.1039/c3nr02105j

Peer reviewed

Published in final edited form as:

*Nanoscale*. 2013 October 7; 5(19): . doi:10.1039/c3nr02105j.

## Carbohydrate-actuated nanofluidic diode: switchable current rectification in a nanopipette

Boaz Vilozny<sup>a</sup>, Alexander L. Wollenberg<sup>a,b</sup>, Paolo Actis<sup>a</sup>, Daniel Hwang<sup>a</sup>, Bakthan Singaram<sup>b</sup>, and Nader Pourmand<sup>a</sup>

Nader Pourmand: pourmand@soe.ucsc.edu

<sup>a</sup>Department of Biomolecular Engineering, Baskin School of Engineering at University of California Santa Cruz, 1156 High Street, Santa Cruz, CA 95064, USA.

<sup>b</sup>Department of Chemistry and Biochemistry, University of California Santa Cruz, 1156 High Street, Santa Cruz, CA 95064, USA

### Abstract

Nanofluidic structures share many properties with ligand-gated ion channels. However, actuating ion conductance in artificial systems is a challenge. We have designed a system that uses a carbohydrate-responsive polymer to modulate ion conductance in a quartz nanopipette. The cationic polymer, a poly(vinylpyridine) quaternized with benzylboronic acid groups, undergoes a transition from swollen to collapsed upon binding to monosaccharides. As a result, the current rectification in nanopipettes can be reversibly switched depending on the concentration of monosaccharides. Such molecular actuation of nanofluidic conductance may be used in novel sensors and drug delivery systems.

### Introduction

Artificial nanopores offer a means to control ion transport, mimicking the behavior of biological ion channels.<sup>1,2</sup> Such solid-state nanopores are at the frontier of single-molecule analytics<sup>3</sup> and offer a window into nanoscale molecular transport.<sup>4,5</sup> In particular, nanofluidic structures with charged surfaces behave as “nanofluidic diodes,” selectively conducting ions of one polarity much like ion channels through a membrane.<sup>6,7</sup> This asymmetric ion transport, or current rectification, generally results from an electrical double layer at charged surfaces, the thickness of which is on the scale of nanofluidic structures. The earliest observation of ion current rectification was seen in 1997 by Wei and Bard, who also observed that at low pH, protonation of anionic surface groups negates the diode-like behavior of quartz nanopipette electrodes.<sup>8</sup> Similar behavior is also seen in asymmetric pores produced by track-etching of polymer films.<sup>9,10,11</sup> This field has now expanded to include many voltage-responsive nanofluidic valves and transistors.<sup>1,12</sup> An intriguing prospect for the development of new nanofluidic devices is to control ion conductance with external stimuli other than voltage, such as small molecules.

Nanofluidic transport can be modulated by a variety of stimuli, including simply changing the concentration gradient of electrolytes.<sup>13</sup> By using chemical receptors, solid-state

© The Royal Society of Chemistry

Correspondence to: Nader Pourmand, pourmand@soe.ucsc.edu.

†Electronic Supplementary Information (ESI) available: Experimental details on synthesis of polymer PVP-Bn, optical methods, 1H-NMR spectra, details on pH and ionic strength studies, and examples of current actuation with several different nanopores. See DOI: 10.1039/b000000x/

nanopores have been engineered to respond to stimuli such as nucleic acids,<sup>14</sup> proteins,<sup>15</sup> small molecules,<sup>16</sup> and metal ions.<sup>17, 18, 19, 20</sup> As with binding of metal ions, the most sensitive and reversible systems are those in which the stimulus modulates surface charge within the nanopores. This is true for pH-responsive nanopores, prepared by attaching acidic or basic moieties onto pore walls and causing current rectification to be modulated with protonation state.<sup>21,22</sup> Greater current modulation can be achieved by incorporating supramolecular chemistry with nanofluidics, such as polyelectrolyte brushes grafted into nanochannels.<sup>23,24,25,26</sup> Such polymer brushes can dramatically alter conductance in response to chemical stimulus by changing charge, hydrophobicity, and conformation. These materials can also respond to non-chemical stimuli such as solvents, heat, and light.<sup>27, 28, 29</sup> Despite these varied modes of stimulus, modulation of nanofluidic transport with uncharged chemical stimuli is still challenging. Such a system would expand the utility of “smart” nanofluidics to include stimuli such as drugs, peptides, and carbohydrates.

Modern techniques to analyze carbohydrates have evolved to meet the needs of blood glucose monitoring,<sup>30</sup> as well as other applications including enzymatic reactions, protein glycosylation, and metabolic profiling.<sup>31,32</sup> Nanopore analytics can be used to detect small molecules using resistive-pulse methods,<sup>1</sup> but the technique is generally more suited to proteins and other macromolecules.<sup>33</sup> Chemically-modified nanopores have been used to analyze mono- and disaccharides, relying on a change in conductance upon saccharide binding. These nanofluidic devices have incorporated biomolecular receptors such as proteins and enzymes.<sup>34, 35, 36</sup> Recently, two groups have independently reported the use of boronic acid receptors in single-channel nanopores.<sup>37,38</sup> The saccharide response in these boronic acid-modified nanopores is a relatively small modulation in current rectification, in contrast to the large modulations achievable with pH-responsive nanopores. This problem may be addressed with new functional materials that can respond to saccharides by changing charge and conformation (Fig. 1), analogous to the response of nanopores modified with pH-responsive polymer brushes.<sup>23,24</sup>

Boronic acids have long been recognized for their ability to reversibly bind carbohydrates.<sup>39</sup> On binding 1,2-diols, the Lewis acidity of the boronic acid is increased (Fig. 2). Binding of carbohydrates results in conversion of the boronic acid to an anionic boronate ester if the  $pK_a$  is shifted to a value lower than the pH of the medium. While most boronic acid-based probes and sensors reported to date use fluorescence,<sup>40</sup> the receptor has also been used for carbohydrate separations,<sup>41</sup> optical sensors based swelling of polymeric materials,<sup>42</sup> and electrochemical sensors.<sup>43</sup> To engineer a saccharide-actuated nanofluidic diode, sought a polyelectrolyte in which the charge is controlled by boronic acid chemistry.

Quartz nanopipettes are nanofluidic structures with intrinsic current rectification,<sup>8</sup> and can be modified using established surface chemistry.<sup>44</sup> Several examples have shown that depositing polycations on the quartz surface reverses the polarity of current rectification.<sup>45,46</sup> The novelty of this work stems from the rational design of a functional polyelectrolyte bearing boronic acid moieties that undergoes a charge-induced conformational change the presence of saccharides. We reasoned that the incorporation of such a polymer into a nanopipette would modulate its permselectivity, as shown in Fig. 1.

Herein we present the synthesis and characterization of a novel boronic acid-containing polycation and its facile incorporation onto nanopipettes. The experimental data presented in this paper confirm our reasoning and show, for the first time, the development of a nanopore turn-on sensor. Furthermore, we elucidate the mechanism of molecular recognition by comparing the behaviour of the functional polyelectrolyte in solution and inside the nanopipette.

## Reagents and Solutions

All stock solutions were prepared in Milli-Q ultrapure water. Reagents were purchased from Sigma Aldrich (St. Louis, Missouri) and used as received. Buffer solutions were prepared from potassium chloride, sodium phosphate dibasic, sodium carbonate, and sodium bicarbonate, and adjusted with either HCl (1 M) or KOH (0.1 M). Alizarin red sulfonate (ARS), L-glucose, and L-fructose were purchased from Sigma Aldrich and used as received. All buffer solutions used for analysis contained 10 mM buffer and 100 mM potassium chloride unless otherwise indicated.

## Synthesis of Polymer PVP-BA

Poly(4-vinylpyridine) (MW 60,000) was purchased from Sigma Aldrich and used as received. The synthesis of *m*-bromomethylphenylboronic acid was carried using an established procedure.<sup>47</sup> To a 10 mL round bottom flask containing a magnetic stir bar were added poly(4-vinylpyridine) (0.100 g, .00167 mmols) and *m*-bromomethyl phenylboronic acid (0.206 g, 0.954 mmols). Then *N,N*-dimethylformamide (2 mL) and methanol (2 mL) were added to dissolve the reagents. The mixture was stirred for 24 hours, then was added dropwise to a 50 mL beaker containing ethyl acetate (10 mL) to precipitate the product. The beaker was placed in an bath to allow the complete precipitation of the product. The solution was then poured into a two-piece fritted filter with removable top and vacuum-filtered under inert conditions using argon gas. The product was washed with 3 × 15 mL portions of ethyl acetate, then left in a vacuum desiccator to dry overnight. Product isolated was 0.257 g (90% yield). As described in the supporting information, <sup>1</sup>H-NMR confirmed the synthesis of poly(4-vinylpyridine) boronic acid (PVP-BA) and showed 80 to 90% alkylation of the polymer.

## Current Measurement with Quartz Nanopipettes

Nanopipettes were fabricated using a P-2000 laser puller (Sutter Instrument Co.) from quartz capillaries with filaments, with an outer diameter of 1.0 mm and an inner diameter of 0.70 mm (QF100-70-5; Sutter Instrument Co.). Parameters used were: Heat 625, Filament 4, Velocity 60, Delay 170, and Pull 180. To measure ion current, a two electrode setup was used. The nanopipette was backfilled with buffer solution (phosphate/KCl, pH 7) and an Ag/AgCl electrode inserted. Another Ag/AgCl electrode was placed in 0.3 mL bulk solution acting as auxiliary/reference electrode. Both electrodes were connected to an Axopatch 700B amplifier with the DigiData 1322A digitizer (Molecular Devices), and a PC equipped with pClamp 10 software (Molecular Devices). To ensure complete wetting of the nanopipette electrodes, nanopipette tips were immersed in *N,N*-dimethylformamide for 5–10 seconds after being backfilled with buffer. Positive potential refers to anodic potential applied to the electrode in the barrel of the nanopipette relative to the counter electrode. Experiments were carried out at 24 °C.

## Modifying Nanopipettes with PVP-BA

Nanopipettes were filled with phosphate buffer (pH 7) and immersed in carbonate buffer (pH 9.5) containing the counter electrode. After verifying the nanopipettes displayed negative current rectification, they were briefly immersed in a methanol solution containing 0.3% (w/v) polymer, then returned to the carbonate solution. Successful immobilization of the polymer resulted in a stable, positively rectified signal.

## Measuring Carbohydrate Response with Polymer-Modified Nanopipettes

Modified nanopipettes were analyzed in 0.30 mL of a carbonate buffer solution (pH 9.5) containing the counter electrode. To the solution were added aliquots of concentrated analyte solutions in pure water. The total volume added did not exceed 15 µL, in order to

limit the change in volume to 5%. To measure response in real time, the current was analyzed using a sinusoidal potential at frequency of 0.5 Hz from  $-500$  to  $+500$  mV. After the signal had stabilized following addition of an aliquot (2–5 min), the current was analyzed by sweeping the voltage from  $-500$  to  $+500$  mV at a rate of  $500$  mV  $s^{-1}$ . Each measurement consisted of 5 sweeps.

### Electrochemical Data Analysis

Ion current measurements recorded with pClamp software (sampling frequency 1000 Hz for voltage sweeps, 200 Hz for sinusoidal function) were imported to OriginPro 8.5 (Origin Labs) for analysis and graphing. To generate I–V curves for each data point, 5 voltage sweeps from  $-800$  to  $+800$  mV at a scan rate of  $500$  mV  $s^{-1}$  were averaged and the standard deviation calculated for each point. To generate binding isotherms, the current at a fixed potential was plotted as a function of analyte concentration.

## Results and discussion

### Chemical properties of the functional polyelectrolyte

Polyelectrolytes were synthesized by quaternization of polyvinylpyridine (Fig. 2). To make a cationic, carbohydrate-actuated polymer, *m*-bromomethylphenylboronic acid was used to alkylate commercially available poly(4-vinylpyridine) (PVP) of molecular weight 60,000. The product, PVP-BA, is weakly soluble in methanol (up to 1% w/v), sparingly soluble in acidic methanol/water solutions, and practically insoluble in other aqueous and organic solvents. A boronic acid-free version of the polymer (PVP-Bn, detailed in supporting information), alkylated with benzyl bromide, showed much higher solubility. The alkylation efficiency of the polymers was determined by integration of  $^1\text{H-NMR}$  spectra (see Figs. S1–S3 in supporting information). Polymer PVP-BA showed 80–90% alkylation, while for PVP-Bn the alkylation efficiency was roughly 90%. These values were used to estimate the molar mass of the polymers as 170,000 for PVP-BA and 150,000 for PVP-Bn. Dynamic light scattering was used to estimate the size of polymer PVP-BA as a dilute solution (0.01%) in methanol/water. This showed a majority of particles with hydrodynamic radius  $R_h$  of 2.2 nm (95%) and two smaller fractions: 6 nm (4%) and 20 nm (1%). Qualitatively, the fraction of larger particles increases with increased salt concentration, though this is difficult to measure due to aggregation/precipitation. We believe these larger particle sizes represent polymer aggregates, and are consistent with reports of  $R_h$  35 nm for quaternized PVP roughly double the length of our polymers measured in 10 mM sodium borate.<sup>48</sup> Polyelectrolytes such as poly(vinylpyridine) can be analyzed by titration to characterize proton uptake.<sup>49</sup> However, the poor solubility of PVP-BA prevented titration analysis to find the apparent  $\text{p}K_a$ .

We titrated an acidified solution of the polymer (1% w/v in 1:1 methanol/water, pH 2) with sodium hydroxide to find the pH at which the polymer precipitates. Presumably, this occurs when a significant portion of the polymer becomes zwitterionic, increasing the hydrophobicity of the molecule.<sup>50,51</sup> This precipitation point was highly reproducible (< 3% RSD for multiple trials), and at pH 7.8 is consistent with the  $\text{p}K_a$  of phenylboronic acid in solution.<sup>52</sup> This precipitation point is modulated in the presence of 20 mM monosaccharides (see Fig. S4 in supporting information), which are known to lower the  $\text{p}K_a$  of boronic acid by as much as 2 pH units.<sup>52</sup> Compared to the precipitation of PVP-BA at  $\text{pH } 7.8 \pm 0.2$ , glucose causes the precipitation to occur at  $\text{pH } 6.5 \pm 0.1$ , and fructose causes precipitation at  $\text{pH } 5.58 \pm 0.08$ . Among monosaccharides, fructose is known to have a high affinity with most monoboronic acid receptors.<sup>52</sup>

## Rectification in polymer-modified nanopipettes

Based on the solution phase experiments, the polymer PVP-BA displays behavior typical of boronic acids, both in terms of pH response and binding to saccharides. We used the limited solubility of the polymer to modify the tip of quartz nanopipettes (pore diameter 30–40 nm). The nanopipettes were filled with pH 7 phosphate buffer in which the polymer is insoluble. Before addition of the polymer, these nanopipettes show almost linear I–V characteristic at pH 7 (Fig. 3B, blue trace). The nanopipette tip was functionalized with PVP-BA by briefly immersing in a methanol solution containing the polymer (0.3% w/v). On returning the nanopipette tip to neutral buffer solution the ion positively rectified (Fig. 3B, red trace). The current rectification is evidence that the polymer interacts with the nanopipette tip, where impedance of the system is highest. Several such polymer-modified nanopipettes were produced by this immersion method, in which the positive rectification was stable over several hours. Presumably, the modified ion current arises from polymer that is embedded in the nanopipette tip, held in place by both electrostatic interaction with the quartz as well as poor solubility in the aqueous solution. Using similar methods, a 20 micron diameter pipette tip showed the polymer confined to a narrow band in the pore region (see Fig. S5 in supporting information).

The pH sensitivity of nanopipettes is considerably enhanced after modification with PVP-BA. As shown in Fig. 4A, the negative rectification before addition of the polymer shows only a slight decrease at pH 3, corresponding to protonation of silanoxy groups. In contrast, the same nanopipette modified with PVP-BA shows highly responsive and nearly ideal diode behavior from pH 8 to pH 3 (Fig. 4B). Significantly, the rectification ratio at low pH ( $I_{\text{open}}/|I_{\text{closed}}|$ ) is as high as 40, comparable to chemically engineered nanofluidic diodes.<sup>6</sup> Comparable diode-like behavior has been observed in DNA-modified nanochannels, attributed to blockage of the pore by electrophoretic movement of polyanions.<sup>53</sup> It is noteworthy that, as shown in Fig. 4B, there is essentially zero ion current for negative potentials with the modified nanopipette. One explanation is in transference of ions across the modified pore. Models of negatively charged, conical glass nanopores indicate there is a high concentration inside the tip of mobile potassium cations due to the electrical double layer. At negative potentials, most of the ion transfer is due to these ions migrating upward toward the negatively biased electrode.<sup>54</sup> In the polymer-modified nanopipettes, immobilized cations of the polymer matrix may replace the mobile potassium cations. Thus, no current would be expected to flow at negative potentials, while at positive potentials the chloride counter-ions of the polymer would account for most ion transfer. A complete picture of these processes requires greater knowledge of the polymer/pore interaction, and likely involves electroosmosis, supramolecular interactions, and acid-base equilibria.

A more detailed analysis of the rectification as a function of pH is shown in Fig. 4B. Rather than immersing the nanopipette in pH-buffered solutions, a bath solution of 100 mM KCl was adjusted using potassium hydroxide from pH 3 to pH 11, and monitored by an external pH meter. The current rectification coefficient  $R_{\text{rect}}$  was plotted as a function of pH, where

$$R_{\text{rect}} = \log(|I_{\text{n}}|/|I_{\text{p}}|)$$

and  $I_{\text{n}}$  and  $I_{\text{p}}$  are the measured current at potentials of  $-500$  mV and  $+500$  mV, respectively. A value of one represents linear (ohmic) behavior with no rectification. The data reveal two inflection points in the current rectification: the first is near pH 4, which may be due to protonation of unalkylated pyridine groups ( $\text{p}K_{\text{a}} \sim 5$ ), which comprise 10–20 % of the polymer chain. The second inflection point is at approximately pH 9.5, a value closer to typical  $\text{p}K_{\text{a}}$  values for phenylboronic acids. The fact that rectification becomes negative at basic pH reveals something about the polymer-modified nanopipette: the current rectification in the pore is not simply governed by replacing a charged quartz surface with a

charged polymer surface. If that were the case, then under basic conditions, the zwitterionic polymer would result in no rectification. Instead, ion permeability appears to be dominated by the polymer at pH values below 10, and by the quartz surface at alkaline conditions above pH 10. To explain that behaviour, it should be noted that not only the charge, but also the solubility of the polymer is highly pH dependent. The positive rectification at low pH may represent a solvated polycation interacting with mobile ions flowing through the pore of the nanopipette, while a zwitterionic polymer at higher pH would be in a collapsed state, having little interaction with electrolytes. This pH-dependent behavior is similar to track-etched nanopores modified with polymer brushes.<sup>24</sup>

In addition to pH, ionic strength is another factor influencing the charge of the polymer. A change in its charge affects the polymer conformation and thus ion conductance in polymer-modified nanopipettes. In solution, the polymer PVP-BA shows lower solubility at higher salt concentrations, likely due to shielding of cationic pyridinium groups by counter-ions, decreasing interaction with the solvent. With modified nanopipettes filled with 0.1 M KCl buffered at pH 7, a strong effect on rectification is seen when immersing in KCl solutions of varying concentration. With the polymer-modified nanopipette, rectification is seen at low ionic strength (0.01 M KCl) and negative rectification with 1.0 M KCl (Fig. 5, and Fig. S6 in supporting information). In contrast, a bare nanopipette consistently shows negative rectification, diminishing with increased ionic strength.<sup>8</sup> This, in addition to the pH-dependent rectification, supports a model where the polymer has a strong effect on ion permeability when in a solvated state, and less influence when it is collapsed, as illustrated in Fig. 1. It should also be noticed, however, that rectification in the 1M salt solution (Fig 5) is more pronounced with the polymer-modified nanopipette than the bare nanopipette. This indicates that even in a collapsed state, the charged polymer has some influence on ion conductance.

### Actuation of Ion Conductance with Carbohydrates

To modulate ion conductance using a saccharide, polymer-modified nanopipettes were immersed in carbonate buffer at pH 9.5, favoring formation of boronate esters.<sup>55</sup> Also, as seen in Fig. 4B, that pH value is near the threshold for modulating ion conductance from positive to negative rectification. The addition of fructose (10 mM) to a polymer-modified nanopipette resulted in rapid inversion of current rectification from positive to negative (Fig. 6A). The response time for complete inversion of current rectification is 3 to 5 minutes. Importantly, the reversal of rectification upon saccharide binding appears identical to that induced at high pH. This points to the same mechanism – conversion of the polymer from the swollen, cationic state to the collapsed, zwitterionic state. At negative potentials, the ion current is dramatically enhanced in the presence of fructose.

At a fixed negative potential, fructose gives a “turn-on” signal that is highly reversible (Fig. 6A and supporting information). Significantly, there are no washing conditions required to restore the signal. The ion conductance at positive potentials is also reversibly actuated with fructose. However, the signal/noise is significantly less. First, the presence of fructose causes a decrease in current at positive potentials, a “turn-off” signal. Second, the high conductance in pure buffer at positive potentials, seen in Fig. 6A, is diminished after initial exposure to the saccharide. This indicates some conditioning of the matrix in the nanopore as a result of carbohydrate binding. While the magnitude of current rectification differed among different polymer-embedded nanopores, the inversion of rectification in the presence of fructose was reversible for several systems tested (see Fig. S7 in the supporting information). In PVP-BA-modified nanopipettes, the polymer plays the role of receptor and actuator while the nanopipette is the transducer. Therefore, it is the binding properties of the polymer that determine the sensitivity system. The dose-response for PVP-BA- modified nanopipettes follows a smooth curve typical of a Langmuir binding isotherm. By plotting

ion current at  $-500$  mV as a function of fructose concentration, a binding affinity can be determined for a given sensor, shown in Equation 1.

$$S = (1 + S_{\max} K_b [A]) / (1 + K_b [A]) \quad (\text{Equation 1})$$

This model uses  $S$  as the signal (ion current),  $S_{\max}$  as the calculated signal upon saturation with analyte,  $[A]$  as the analyte concentration, and  $K_b$  as the binding constant in units of  $M^{-1}$ . The binding constant for fructose determined from the isotherm in Fig. 6B is  $360 \pm 110 M^{-1}$ . This affinity is in the range typical of phenylboronic acids, which vary from 100 to  $5000 M^{-1}$ .<sup>52</sup>

The anionic catechol alizarin red sulfonate (ARS) is commonly used as an indicator for boronic acids. This dye has two mechanisms for binding to the polymer PVP-BA. The catechol group has a high affinity with boronic acids, and there is also electrostatic attraction between the cationic polymer and anionic dye. When tested with a PVP-BA modified nanopipette, low concentrations of ARS caused shifts in current rectification only seen with much greater concentrations of fructose. As shown in Fig. 7A, as little as  $60 \mu M$  ARS is sufficient to negate all positive rectification. With  $360 \mu M$  ARS, the current is negatively rectified. This high sensitivity (relative to fructose) can be explained by an enhanced affinity between PVP-BA and ARS.

By observing the absorbance spectrum of the dye in bulk solution (Fig. 7B), we see a distinct effect for PVP-BA binding not observed with PVP-Bn, the polymer lacking boronic acids. In the presence of PVP-Bn, the absorbance maximum at  $420$  nm decreases and is slightly red-shifted to  $432$  nm. When PVP-BA is added to the dye, the maximum absorbance increases and is shifted to  $467$  nm. These absorbance changes reflect an interaction due to both boronic acid binding and electrostatic interactions. At low concentrations of ARS ( $< 0.1$  mM), the modulation of ion current rectification is completely reversible, requiring no washing media (see supporting information, Fig. S8.). Higher concentrations caused the system to become permanently negatively rectified. This may be due to strong interactions between the polymer and the dye, especially if the dye penetrates into the polymer matrix and is prevented from diffusing into the bulk solution.

## Conclusions

In this work a quartz nanopipette was modified with a saccharide-binding polymer, resulting in a switchable nanofluidic diode. Notably, modification of the nanopipette required only immersing in a polymer solution, rather than chemical conjugation. We elucidated the mechanism of actuation of ion current by comparing the behaviour of the polymer in solution and after conjugation in the nanopipette. The mechanism relied on charge induced swelling and collapse of the polymer in response to the presence of saccharide. This method resulted in the development of the first turn-on nanopore sensor. This technique could be used to engineer feedback-controlled delivery systems for ions or other particles. To tune the selectivity of the device for different carbohydrates, the configuration of the boronic acid receptor<sup>56</sup> can be varied, along with the composition and charge of the polymer matrix.<sup>57</sup> While we have focused here on chemical modulation of nanofluidic conductance, nanopores with chemical selectivity are often used in resistive-pulse sensing (single-molecule counting).<sup>58,59,60</sup> Thus, we believe the method of controlling nanofluidic transport with a functional polymer matrix will find use in single-molecule analytical techniques.

## Supplementary Material

Refer to Web version on PubMed Central for supplementary material.



## Acknowledgments

We thank Prof. Holger Schmidt and Dr. Tom Yuzvinsky of the Keck Center for Nanoscale Optofluidics at UC Santa Cruz for electron microscopy of the nanopores. This work was supported in part by grants from the National Cancer Institute [U54CA143803], and the National Institutes of Health [P01-35HG000205]

## References

1. Siwy ZS, Howorka S. *Chem. Soc. Rev.* 2010; 39:1115–1132. [PubMed: 20179828]
2. Hou X, Guo W, Jiang L. *Chem. Soc. Rev.* 2011; 40:2385–2401. [PubMed: 21308139]
3. Howorka S, Siwy Z. *Chem. Soc. Rev.* 2009; 38:2360–2384. [PubMed: 19623355]
4. Keyser UF. *J. Royal Soc. Interface.* 2011
5. Kowalczyk SW, Kapinos L, Blosser TR, Magalhaes T, van Nies P, Lim RYH, Dekker C. *Nat Nano.* 2011; 6:433–438.
6. Vlasiouk I, Siwy ZS. *Nano Lett.* 2007; 7:552–556. [PubMed: 17311462]
7. Cheng L-J, Guo LJ. *Chem. Soc. Rev.* 2010; 39:923–938. [PubMed: 20179815]
8. Wei C, Bard AJ, Feldberg SW. *Anal. Chem.* 1997; 69:4627–4633.
9. Siwy Z, Gu Y, Spohr HA, Baur D, Wolf-Reber A, Spohr R, Apel P, Korchev YE. *EPL (Europhysics Letters).* 2002; 60:349.
10. Siwy Z, Apel P, Dobrev D, Neumann R, Spohr R, Trautmann C, Voss K. *Nucl. Instrum. Meth. Phys. Res. B.* 2003; 208:143–148.
11. Siwy Z, Apel P, Baur D, Dobrev DD, Korchev YE, Neumann R, Spohr R, Trautmann C, Voss K-O. *Surf. Sci.* 2003; 532–535:1061–1066.
12. Powell MR, Cleary L, Davenport M, Shea KJ, Siwy ZS. *Nat Nano.* 2011; 6:798–802.
13. Wanunu M, Morrison W, Rabin Y, Grosberg AY, Meller A. *Nat Nano.* 2010; 5:160–165.
14. Fu Y, Tokuhisa H, Baker LA. *Chem Commun(Cambridge, U.K.).* 2009:4877–4879.
15. Ali M, Yameen B, Neumann R, Ensinger W, Knoll W, Azzaroni O. *J. Am. Chem. Soc.* 2008; 130:16351–16357. [PubMed: 19006302]
16. Actis P, Jejelowo O, Pourmand N. *Biosens. Bioelectron.* 2010; 26:333–337. [PubMed: 20829024]
17. Sa N, Fu Y, Baker LA. *Anal. Chem.* 2010; 82:9963–9966. [PubMed: 21090777]
18. Actis P, Vilozny B, Seger RA, Li X, Jejelowo O, Rinaudo M, Pourmand N. *Langmuir.* 2011; 27:6528–6533. [PubMed: 21510657]
19. Vilozny B, Actis P, Seger RA, Vallmajo-Martin Q, Pourmand N. *Anal. Chem.* 2011; 83:6121–6126. [PubMed: 21761859]
20. Actis P, McDonald A, Beeler D, Vilozny B, Millhauser G, Pourmand N. *RSC Advances.* 2012
21. Wanunu M, Meller A. *Nano Lett.* 2007; 7:1580–1585. [PubMed: 17503868]
22. Ali M, Ramirez P, Mafé S, Neumann R, Ensinger W. *ACS Nano.* 2009; 3:603–608. [PubMed: 19222230]
23. Yameen B, Ali M, Neumann R, Ensinger W, Knoll W, Azzaroni O. *Chem. Commun. (Cambridge).* 2010; 46:1908–1910. [PubMed: 20198249]
24. Yameen B, Ali M, Neumann R, Ensinger W, Knoll W, Azzaroni O. *Nano Lett.* 2009; 9:2788–2793. [PubMed: 19518086]
25. Yameen B, Ali M, Neumann R, Ensinger W, Knoll W, Azzaroni O. *J. Am. Chem. Soc.* 2009; 131:2070–2071. [PubMed: 19159287]
26. Tagliazucchi M, Azzaroni O, Szleifer I. *J. Am. Chem. Soc.* 2010; 132:12404–12411. [PubMed: 20718436]
27. Azzaroni O. *J. Polym. Sci. A.* 2012; 50:3225–3258.
28. Peleg O, Tagliazucchi M, Kröger M, Rabin Y, Szleifer I. *ACS Nano.* 2011; 5:4737–4747. [PubMed: 21524134]
29. Lim RYH, Deng J. *ACS Nano.* 2009; 3:2911–2918. [PubMed: 19728698]
30. Vashist SK, Zheng D, Al-Rubeaan K, Luong JHT, Sheu F-S. *Anal. Chim. Acta.* 2011; 703:124–136. [PubMed: 21889626]

31. Kraly JR, Holcomb RE, Guan Q, Henry CS. *Anal. Chim. Acta.* 2009; 653:23–35. [PubMed: 19800473]
32. An HJ, Kronewitter SR, de Leoz MLA, Lebrilla CB. *Curr. Opin. Chem. Biol.* 2009; 13:601–607. [PubMed: 19775929]
33. Bacri L, Oukhaled A, Hémon E, Bassafoula FB, Auvray L, Daniel R. *Biochem. Biophys. Res. Commun.* 2011
34. Tripathi A, Wang J, Luck LA, Suni II. *Anal. Chem.* 2006; 79:1266–1270. [PubMed: 17263364]
35. Fink D, Klinkovich I, Bukelman O, Marks RS, Kiv A, Fuks D, Fahrner WR, Alfonta L. *Biosens. Bioelectron.* 2009; 24:2702–2706. [PubMed: 19138511]
36. Ali M, Ramirez P, Tahir MN, Mafe S, Siwy Z, Neumann R, Tremel W, Ensinger W. *Nanoscale.* 2011; 3:1894–1903. [PubMed: 21423941]
37. Nguyen QH, Ali M, Neumann R, Ensinger W. *Sens. Actuators B.* 2012; 162:216–222.
38. Sun Z, Han C, Wen L, Tian D, Li H, Jiang L. *Chem. Commun. (Cambridge, U.K.).* 2012; 48:3282–3284.
39. Lorand JP, Edwards JO. *J. Org. Chem.* 1959; 24:769–774.
40. Mader HS, Wolfbeis OS. *Microchim. Acta.* 2008; 162:1–34.
41. Nishiyabu R, Kubo Y, James TD, Fossey JS. *Chem. Commun. (Cambridge, U.K.).* 2011; 47:1106–1123.
42. Cambre JN, Sumerlin BS. *Polymer.* 2011; 52:4631–4643.
43. Park S, Boo H, Chung TD. *Anal. Chim. Acta.* 2006; 556:46–57. [PubMed: 17723330]
44. Actis P, Mak A, Pourmand N. *Bioanal. Rev.* 2010; 1:177–185. [PubMed: 20730113]
45. Liu S, Dong Y, Zhao W, Xie X, Ji T, Yin X, Liu Y, Liang Z, Momotenko D, Liang D, Girault HH, Shao Y. *Anal. Chem.* 2012; 84:5565–5573. [PubMed: 22762260]
46. Umehara S, Pourmand N, Webb CD, Davis RW, Yasuda K, Karhanek M. *Nano Lett.* 2006; 6:2486–2492. [PubMed: 17090078]
47. Gamsey S, Baxter NA, Sharrett Z, Cordes DB, Olmstead MM, Wessling RA, Singaram B. *Tetrahedron.* 2006; 62:6321–6331.
48. Sybachin AV, Efimova AA, Litmanovich EA, Menger FM, Yaroslavov AA. *Langmuir.* 2007; 23:10034–10039. [PubMed: 17718526]
49. Tantavichet N, Pritzker MD, Burns CM. *J. Appl. Polym. Sci.* 2001; 81:1493–1497.
50. Chen W, Pelton R, Leung V. *Macromolecules.* 2009; 42:1300–1305.
51. Ivanov AE, Shiomori K, Kawano Y, Galaev IY, Mattiasson B. *Biomacromolecules.* 2006; 7:1017–1024. [PubMed: 16602716]
52. Yan J, Springsteen G, Deeter S, Wang B. *Tetrahedron.* 2004; 60:11205–11209.
53. Harrell CC, Kohli P, Siwy Z, Martin CR. *J. Am. Chem. Soc.* 2004; 126:15646–15647. [PubMed: 15571378]
54. White HS, Bund A. *Langmuir.* 2008; 24:2212–2218. [PubMed: 18225931]
55. Duggan PJ, Offermann DA. *Tetrahedron.* 2009; 65:109–114.
56. Gamsey S, Miller A, Olmstead MM, Beavers CM, Hirayama LC, Pradhan S, Wessling RA, Singaram B. *J. Am. Chem. Soc.* 2007; 129:1278–1286. [PubMed: 17263411]
57. Ancla C, Lapeyre V, Gosse I, Catargi B, Ravaine V. *Langmuir.* 2011; 27:12693–12701. [PubMed: 21892832]
58. Sexton LT, Mukaibo H, Katira P, Hess H, Sherrill SA, Horne LP, Martin CR. *J. Am. Chem. Soc.* 2010; 132:6755–6763. [PubMed: 20411939]
59. Yusko EC, Johnson JM, Majd S, Prangkio P, Rollings RC, Li J, Yang J, Mayer M. *Nat Nano.* 2011; 6:253–260.
60. Li W, Bell NAW, Hernández-Ainsa S, Thacker VV, Thackray AM, Bujdoso R, Keyser UF. *ACS Nano.* 2013; 7:4129–4134. [PubMed: 23607870]

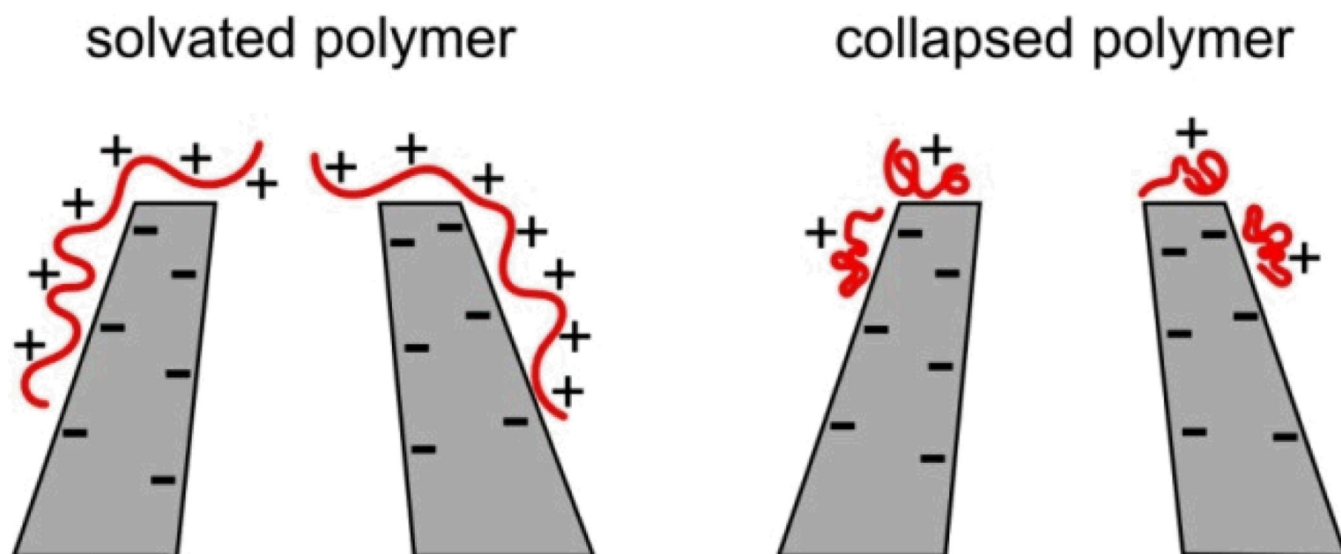


**Fig. 1.** Both conformation and charge of immobilized polymers influence ion transport through a nanopipette. Compared with a swollen cation at the pore, a collapsed polymer will effect less the ion conductance.

# Experimental Section

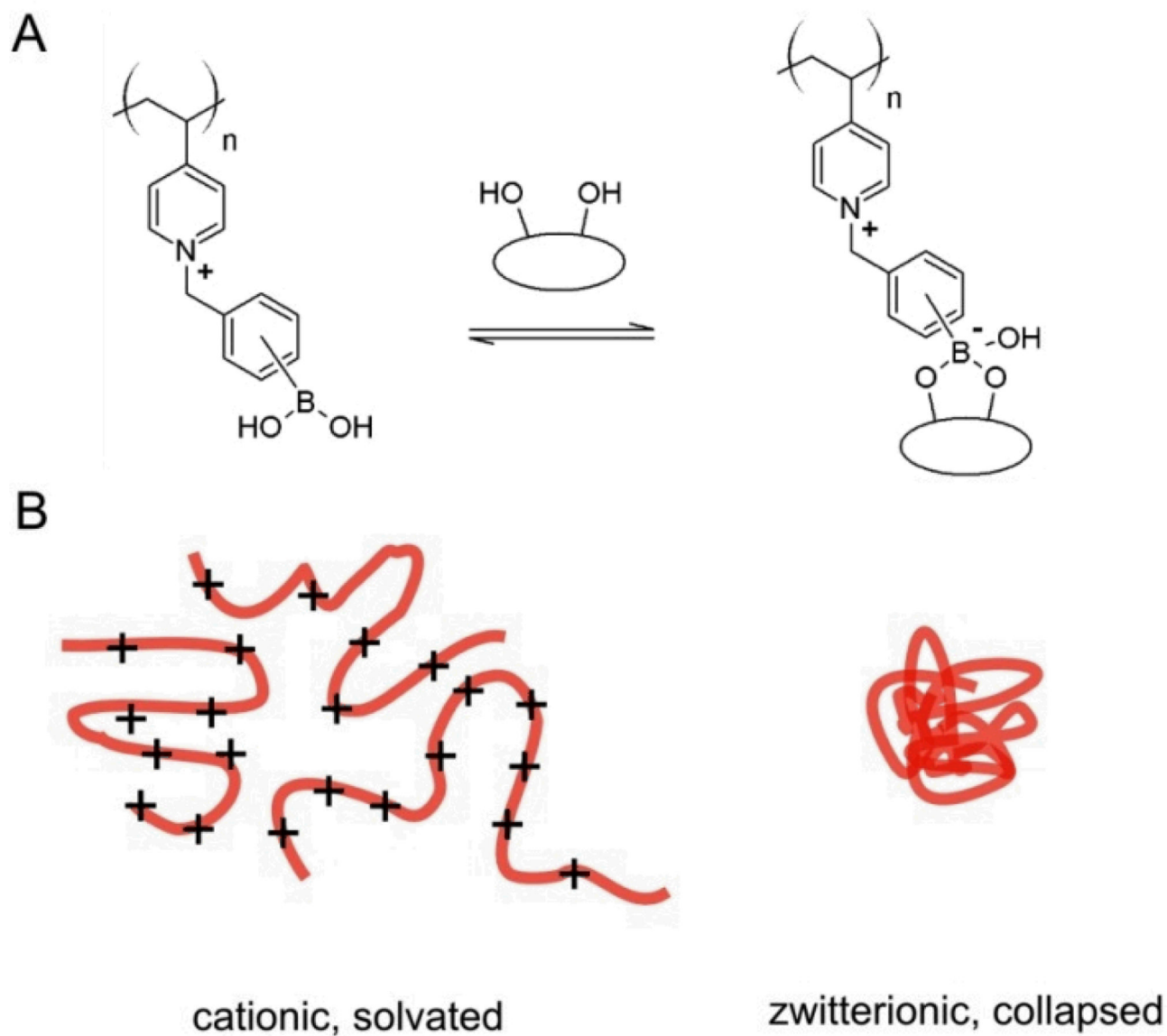


**Fig. 2.** Saccharide binding by polymer PVP-BA causes changes in charge and conformation. (A) The cationic polymer is neutralized when carbohydrates bind to the boronic acid unit. (B) The hydrophobic polymer is insoluble in the zwitterionic state.

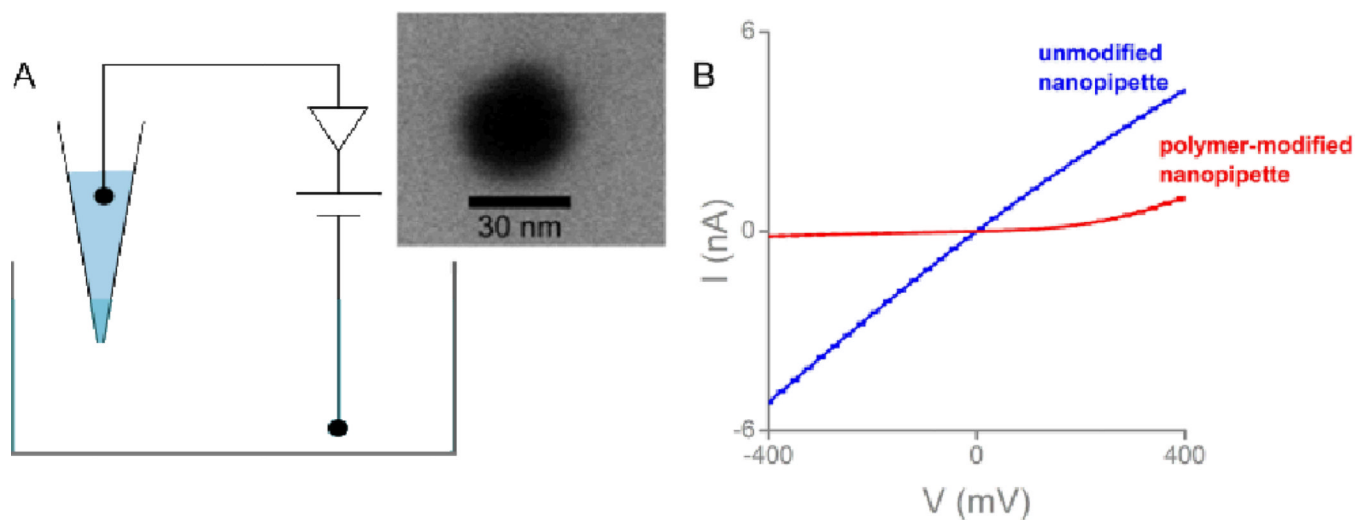


**Fig. 3.** Current rectification changes with polymer modification of nanopipettes. (A) Electrochemical setup with a working electrode inside the nanopipette barrel and counter electrode in the bath solution. (B) Ion current rectification at pH 7 for a nanopipette before (blue) and after (red) modification with polymer PVP-BA. Error bars reflect standard deviation from 5 voltage scans. Inset: Scanning electron micrograph of a quartz nanopipette tip.

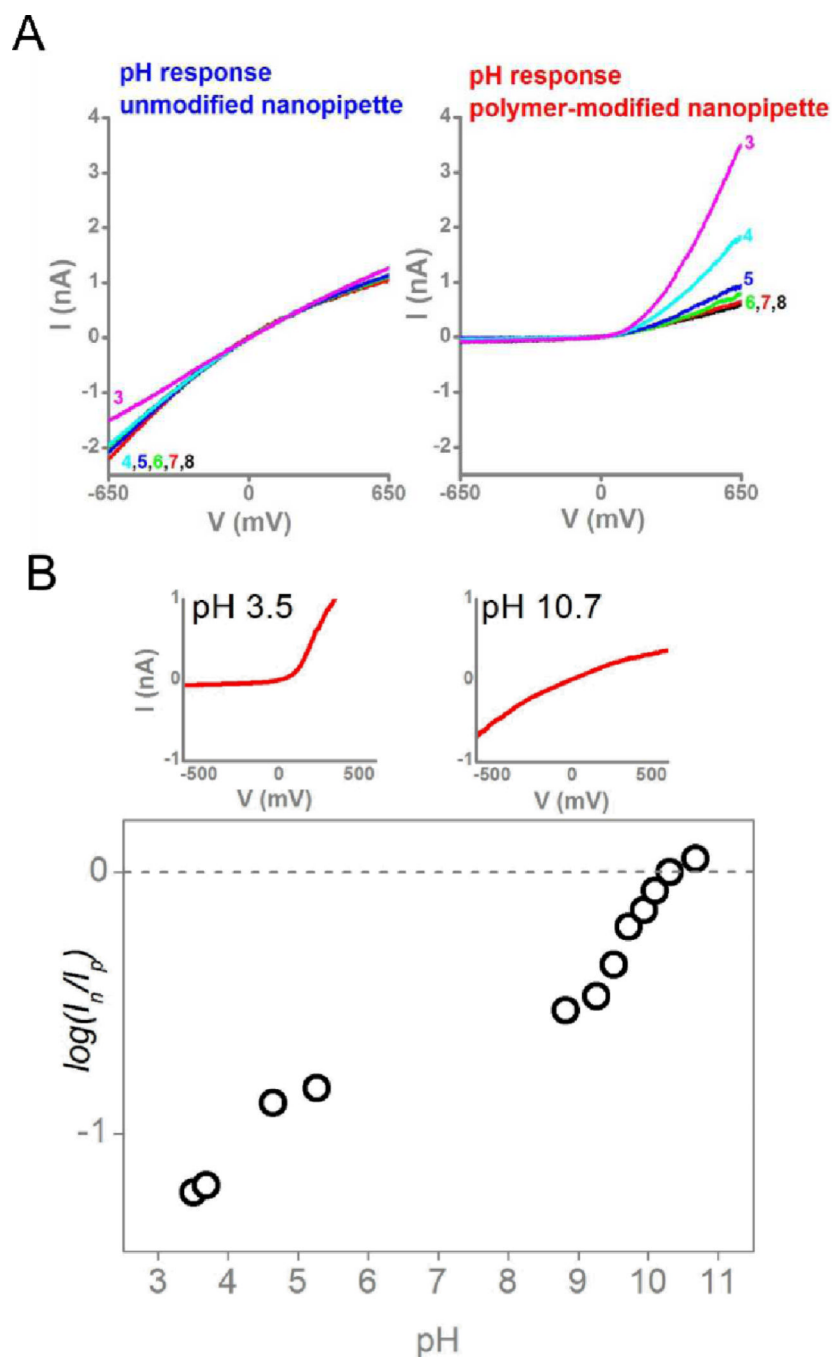


**Fig. 4.** Polymer-modified nanopipettes are highly pH-sensitive. Response from an unmodified nanopipette before (top left panel) and after (red top right panel) modification with PVP-BA. The nanopore was filled with phosphate buffer (pH 7) and immersed in phosphate/citrate buffers from pH 3 to pH 8 in increments of one pH unit. (B) Rectification response of a PVP-BA-modified nanopipette immersed in unbuffered 100 mM KCl, with pH measured by external pH-meter. Solution pH was adjusted with NaOH. The two insets show I–V curves with positive rectification at low pH (left) and negative rectification at high pH (right)

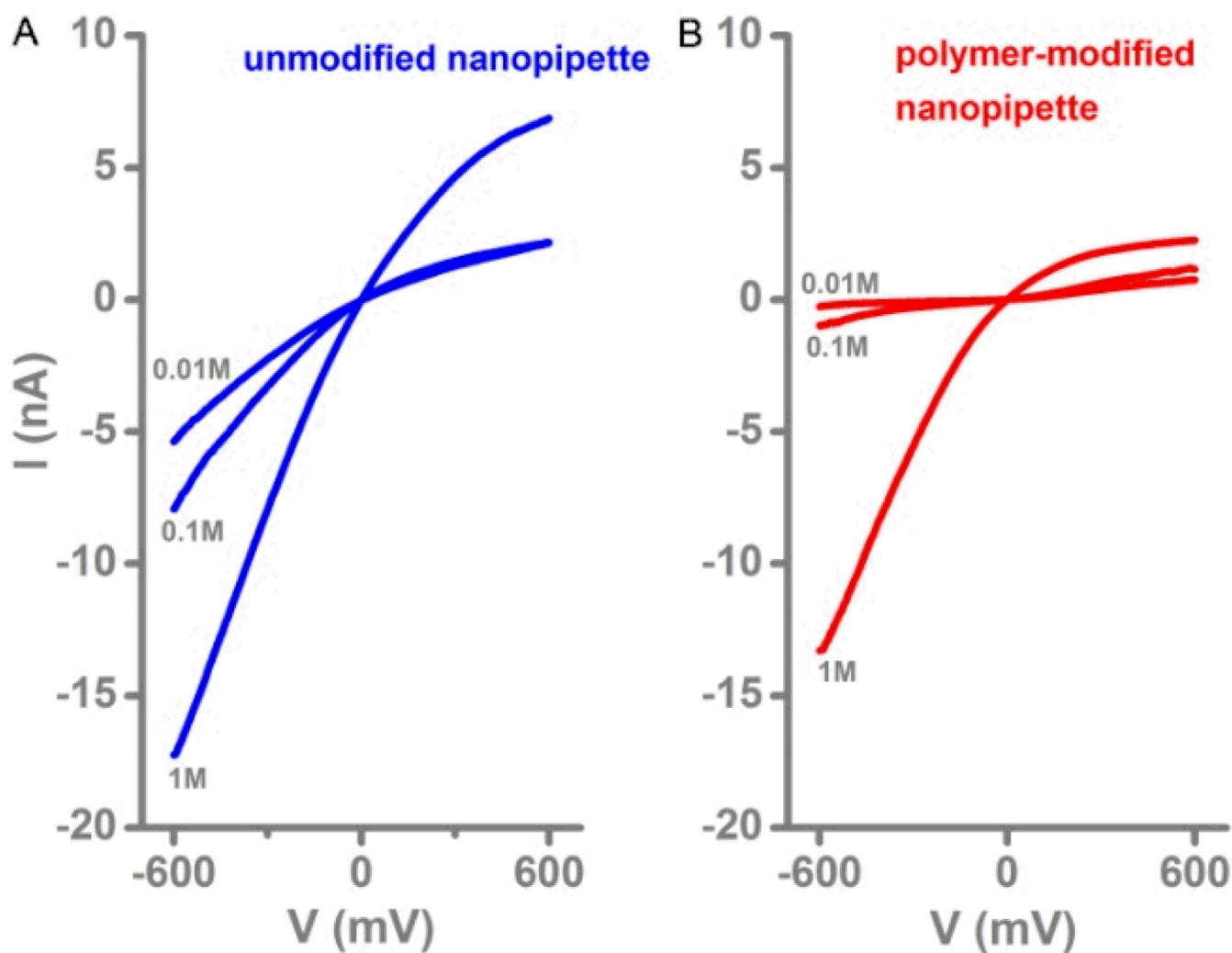


**Fig. 5.** Polymer-modified nanopipettes show distinct response to ionic strength. I–V curves are shown for unmodified (A) and PVP-BA-modified (B) nanopipette electrodes. Nanopipettes were filled with phosphate buffer (10 mM potassium phosphate, pH 7; 0.1 M KCl) and immersed in similar buffer containing either 0.01, 0.1, or 1.0 M KCl as specified in the graphs.

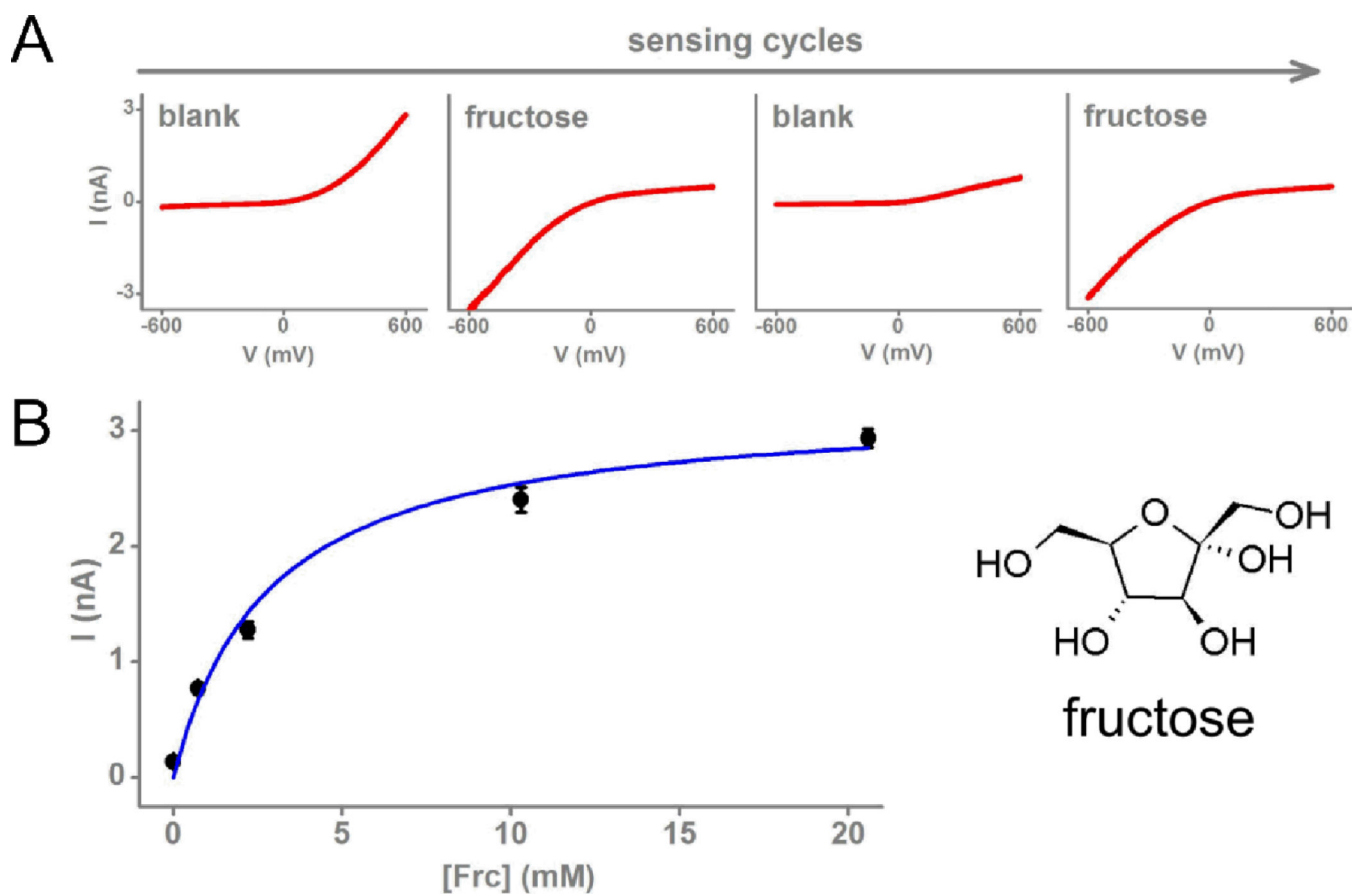


**Fig. 6.** Polymer-modified nanopipettes respond reversibly to fructose. **(A)** Sequential current-voltage curves for a nanopipette immersed in pH 9.5 carbonate buffer with either zero or 10 mM fructose. **(B)** Binding isotherm showing ion current (absolute value) measured at  $-0.5$  V with increasing fructose concentration. Error bars show the standard deviation from repeated voltage scans ( $N=5$ ). The best fit line is shown for Equation 1, with a binding constant  $K_b$  determined to be  $360 \pm 110$  M



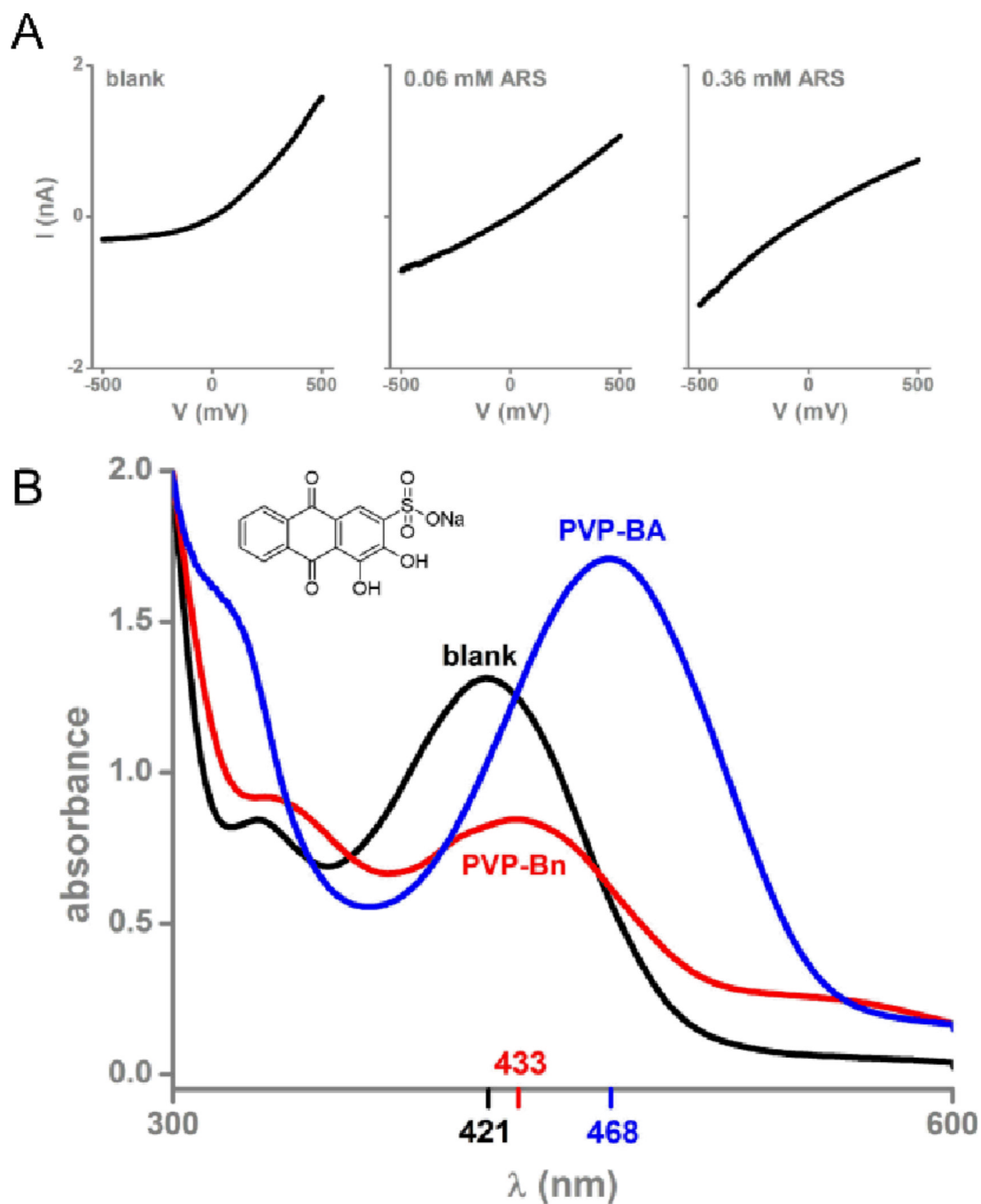


**Fig. 7.**

An anionic catechol shows especially high affinity for polymer PVP-BA. (A) Modulation of ion permeability through a PVP-BA modified nanopipette in the presence of ARS (structure shown). The nanopipette electrode was immersed in pH 9.5 carbonate buffer containing 0, 0.06, or 0.36 mM ARS. (B) Absorbance spectra of ARS alone (black) and with addition of polymers PVP-BA (blue) and PVP-Bn (red) at 200 ppm polymer concentration. The dye solution is 0.25 mM ARS in 1:1 methanol/water.